

AD-A091 646

GEORGETOWN UNIV WASHINGTON D C DEPT OF PHYSICS

F/6 20/1

MEASUREMENT OF THE HARMONIC CONTENT ACROSS A BOUNDED ULTRASONIC--ETC(U)

OCT 80 D D MCLENNAN

N00014-78-C-0584

UNCLASSIFIED

GUUS-108003

NL

1-1-1
AL
ADONIS 36



END
DATE
FILMED
12-80
DTIC



LEVEL II

(12)

OFFICE OF NAVAL RESEARCH

CONTRACT N00014-78-C-0584

(15)

(9) Master Copy
Technical Report No. 3
1 Apr 79

AD A091646

(6) MEASUREMENT OF THE HARMONIC CONTENT ACROSS A
BOUNDED ULTRASONIC BEAM.

DTIC
ELECTE
NOV 18 1980
E

(10) by
Douglas D. McLennan

(14) GUS-108003, TR-3

Tran D.K. Ngoc
Co-Principal Investigator
Department of Physics
Georgetown University
Washington, DC 20057

(11) Oct 1980 (253)

Approved for Public Release. Distribution Unlimited

DDC FILE COPY

80 10 31 028
152620

UNCLASSIFIED

SECURITY CLASSIFICATION OF THIS PAGE (When Data Entered)

REPORT DOCUMENTATION PAGE		READ INSTRUCTIONS BEFORE COMPLETING FORM
1. REPORT NUMBER GUUS 108003	2. GOVT ACCESSION NO. AD-A091646	3. RECIPIENT'S CATALOG NUMBER
4. TITLE (and Subtitle) Measurement of the Harmonic Content across a Bounded Ultrasonic Beam	5. TYPE OF REPORT & PERIOD COVERED Technical 1 April 1980-15 Oct. 1980	
	6. PERFORMING ORG. REPORT NUMBER TR3	
7. AUTHOR(s) Douglas D. McLennan	8. CONTRACT OR GRANT NUMBER(s) N00014-78-C-0584	
9. PERFORMING ORGANIZATION NAME AND ADDRESS Physics Department Georgetown University Washington, DC 20057	10. PROGRAM ELEMENT, PROJECT, TASK AREA & WORK UNIT NUMBERS 121108	
11. CONTROLLING OFFICE NAME AND ADDRESS Office of Naval Research, Code 421 Arlington, Virginia 22217	12. REPORT DATE 22 October 1980	
	13. NUMBER OF PAGES 53	
14. MONITORING AGENCY NAME & ADDRESS (if different from Controlling Office)	15. SECURITY CLASS. (of this report) Unclassified	
	15a. DECLASSIFICATION/DOWNGRADING SCHEDULE	
16. DISTRIBUTION STATEMENT (of this Report) Approved for public release; distribution unlimited.		
17. DISTRIBUTION STATEMENT (of the abstract entered in Block 20, if different from Report) Approved for public release; distribution unlimited.		
18. SUPPLEMENTARY NOTES		
19. KEY WORDS (Continue on reverse side if necessary and identify by block number) Ultrasonics, harmonic generation, finite source, nonlinear interaction, attenuation, diffraction.		
20. ABSTRACT (Continue on reverse side if necessary and identify by block number) An experimental technique is designed to map the fundamental and harmonic sound amplitudes across a bounded beam for different distances from the source. The measured profiles reflect the in- fluences of competing mechanisms such as nonlinearity, dissipation, and diffraction in a liquid medium.		

DD FORM 1 JAN 73 1473

EDITION OF 1 NOV 65 IS OBSOLETE
S/N 0102-014-6601

Unclassified

SECURITY CLASSIFICATION OF THIS PAGE (When Data Entered)

This Technical Report describes the work done by Douglas D. McLennan for his M.Sc. degree in physics at Georgetown University. This effort is part of the project supported by the Office of Naval Research, Physics Program (Code 421), under Contract N00014-78-C-0584.

The study is an experimental investigation of the harmonic composition of a bounded ultrasonic beam. The frequency-sensitive technique employed to measure the sound amplitude allows one to map separate acoustic profiles for the fundamental and each harmonic component. The constituent profiles are determined for sound waves of a fundamental frequency 3MHz generated by a finite source having a 2cm diameter. It is observed that the measured constituent profiles change as the sound waves travel away from the source. These changes represent the competing influences of several mechanisms such as nonlinearity, diffraction, and dissipation which are known to be present in any liquid medium.

Tran D.K. Ngoc

Co-Principal Investigator

October 1980

Accession For	
NTIS GRA&I	<input checked="checked" type="checkbox"/>
DDC TAB	<input type="checkbox"/>
Unannounced	<input type="checkbox"/>
Justification	
By _____	
Distribution/_____	
Availability Codes	
Dist.	Avail and/or special
A	

CHAPTER I

INTRODUCTION

Acoustic wave propagation is an inherently nonlinear process. The nonlinearity manifests itself via the generation of harmonics as an acoustic wave travels through a medium. The specific problem studied here is further complicated by the fact that the source is finite. Thus a theoretical description of this process involves a nonlinear differential equation with boundary conditions appropriate to a finite dimensional source.

The theoretical foundations of nonlinear acoustics were developed by Euler [1] during the mid-eighteenth century. It was not until the middle of the nineteenth century though, that the implications of the theory of nonlinear acoustic plane wave propagation were understood [2]. The current theoretical models have expanded upon the early simple plane wave theory in an effort to describe many of the complexities present in nature such as dissipation, diffraction, interference as well as the production of harmonics as an initially sinusoidal wave travels through a nonlinear medium [3,4].

In the 1950's experimental evidence of harmonic generation in acoustic beams was seen in the form of asymmetric

light diffraction patterns produced when high-intensity ultrasonic waves interacted with monochromatic light [5]. The first experimental identification of the higher harmonics generated within ultrasonic waves was accomplished by Krasilnikov et al [6]. More recently, maps of the harmonic content of sound fields have been made for large distances from the source and for relatively low ultrasonic frequencies [7,8].

The experimental investigation of the nonlinear production of harmonics as presented here involves measurements of ultrasonic waves of low-MHz frequencies propagating in water. The reasons for using this frequency range are twofold. First, the use of low-MHz frequencies reduces the acoustic wavelength so as to facilitate measurements of a laboratory scale. Second, much medical and scientific work is done using ultrasonic waves in the 1 to 10 MHz range. The measurements were made at distances ranging from 15 to 25 cm from a 2 cm diameter circular source. At each distance an amplitude map of the fundamental and the first two harmonics was recorded using a miniature hydrophone. The frequency response of the hydrophone was measured so that the amplitudes of the individual frequencies could be compared.

The presentation of the work done here begins with

a brief description of the theoretical background and a review of some of the experimental techniques used in measuring ultrasonic waves. The particular experimental apparatus along with the calibration procedure is then discussed. Finally the experimental results and discussion are presented.

CHAPTER II

THEORETICAL BACKGROUND

A simple one-dimensional equation of motion for an acoustic wave in a fluid is given by [2]

$$\left(1 + \frac{\partial \xi}{\partial x}\right)^2 \frac{\partial^2 \xi}{\partial t^2} = c_0^2 \frac{\partial^2 \xi}{\partial x^2} \quad (2.1)$$

where c_0 is the propagation speed and ξ is the particle displacement from its equilibrium position. Equation (2.1) ignores many of the complexities present in nature such as dissipation, diffraction, and interference. But, the presence of the term in brackets on the left-hand side of equation (2.1) makes it a nonlinear wave equation. Physically, the nonlinearity of acoustic wave motion is caused by the properties of the medium through which the wave travels. First, since the wave in a fluid is longitudinal, a particle set in motion by the passage of the wave contributes its own velocity to the velocity of the wave. Second, the relationship between pressure and density is not a simple linear one. The former effect dominates in gases while the latter dominates in liquids [9]. The overall effect is that, within the wave compressions travel faster than rarefactions and an initially sinusoidal acoustic waveform distorts as it propagates

through the medium [1].

It should be noted that equation (2.1) reduces to an ordinary wave equation if ($\partial \xi / \partial x$) were to be neglected, in which case a solution of the form

$$\xi = \xi_0 \sin(\omega t - bx) \quad (2.2)$$

would satisfy equation (2.1). This would imply that the wave velocity would be the same for any frequency and would be constant, regardless of the value of ξ_0 , the maximum particle displacement. However, it is obvious that for any real acoustic wave the spatial rate of change of the particle displacement, ($\partial \xi / \partial x$), is not zero and the wave has a finite amplitude (as opposed to an infinitesimal amplitude when one assumes that ($(\partial \xi / \partial x) \rightarrow 0$), leading to "finite-amplitude distortions".

During the early part of the nineteenth century both Poisson and Lagrange [1] obtained proof of these distortions phenomena but were reluctant to believe their own findings. Lagrange commented that "the new formula would destroy the uniformity of the speed of sound and would make it depend in some ways on the nature of the original disturbance: that which is contrary to all experiments". Poisson questioned the validity of his findings and stated that all sound, loud or faint is transmitted with same speed".

In 1848 the British physicist Stokes interpreted the implications of nonlinear wave propagation and pointed out that the wave becomes progressively distorted as it propagates through the medium and eventually reaches a point where the slope of the leading edge of the waveform becomes infinite, hence a shock wave is formed.

An equation similar to (2.1) was solved in implicit form by Earnshaw in 1859 [2] and an exact solution to Earnshaw's formulation was found by Fubini in 1935 [2].

The distortion of a sinusoidal waveform, which will occur when $(\partial \xi / \partial x) \neq 0$, manifests itself via the generation of harmonics as the wave travels through the medium. Thus a Fourier analysis of a distorted waveform contains the original fundamental frequency and higher harmonics, with the higher harmonics being continually added to the fundamental until the original sinusoidal wave becomes a saw-tooth wave. This is in keeping with the results of the velocity analysis of equation (2.1) which predicts that the high compression portion of the wave travels faster than the rarefaction, eventually causing the waveshape to become a saw-tooth.

This holds true for dissipationless media. But fluids dissipate acoustic intensity, primarily due to absorption.

In most fluids the absorption coefficient is proportional to the square of the frequency. This effectively prevents shock formation as the very high harmonics are attenuated faster than they are produced [2].

It becomes necessary, therefore, that attenuation be considered in an analysis of acoustic wave motion. In 1931 Fay [2] developed a theory of the "almost stable waveform" which showed that nonlinear harmonic generation is eventually balanced by absorption after a certain travel distance.

A combined use of fluid dynamics and wave mechanics led to the development of the so-called generalized Burgers equation, which takes into account major phenomena such as diffraction and absorption in addition to nonlinearity [3]. Analytical solutions to this equation have been obtained for plane waves travelling in an isotropic medium [10]. Other nonlinear acoustic wave equations which take into account absorption as well as finite source dimensions have also been derived [3,4]. Numerical solutions to some of these equations have been computed [11,12], showing the progression growth of the harmonics, but failing to show any interference effects expected when considering a source of finite dimensions in the near field

range.

Although general trends are predicted by simple models as described by equation (2.1), the experimental measurements made here have no theoretical model against which they can be compared. The major theoretical obstacle encountered involves solving the nonlinear equation that incorporates a finite-dimension source.

Theoretical descriptions exist for both an infinite source (plane wave theory) and a point source. But, the measurements here were made sufficiently far from the source so as to exclude the latter description.

The experimental measurements made here exemplify both the nonlinear nature of acoustic wave motion and the effects of finite source dimensions. It is hoped that these measurements will provide a basis for further theoretical work so that it will be possible to determine the contribution of either of these processes to the observed effects.

CHAPTER III

EXPERIMENTAL TECHNIQUES

Measurements of ultrasonic beams with the purpose of producing a plot of both the intensity and the spectral content put various constraints upon the particular technique to be used. As with any measuring technique, one desires a minimum of interference by the measuring device on the system, a technique that is easily calibrated, and an apparatus whose sensitivity fall within the limits of a given application. Thus it is evident that some work is involved in the design and calibrating of an apparatus which will allow one to measure the beam profile and the frequency distribution in the beam.

There are many methods in use today for measuring ultrasonic fields [13]. A short review of some of these methods will be given paying special attention to the particular needs of the present experiment.

1. Acoustic Pressure

A straightforward method for determining acoustic intensity consists of measuring the radiation force on a target of reflecting or absorbing material. For a progressive ultrasonic wave impinging upon a perfectly absorbing target, the acoustic power is equal to the

product of force times the speed of sound [14]. Although this technique usually uses large targets to measure total ultrasonic power [13], a sphere suspended on a pendulum could be used to determine the profile of a beam [15]. The advantage of the radiation force method is the ease of calibration [14]. But, since one is measuring time-integrated radiation force, the method is totally insensitive to the spectral content of the beam.

2. Thermal

Another method for determining ultrasonic intensities involves measuring the thermal energy the acoustic beam deposits in an absorbing medium. The resulting temperature rise is compared to a known source of thermal energy. Thus, the system measures the time-measured mechanical energy flow of the sound beam. Here again, this technique is totally insensitive to the spectral content of the beam.

3. Interferometric

A much more complicated system used to measure ultrasonic fields involves optical interferometry. In this system, a Michelson interferometer is set up with one of its legs containing an optically transparent flexible mirror. The mirror is placed in the ultrasonic sound field. Distortions across the face of the mirror are proportioned to

the particle displacement in the ultrasonic field. The mirror is scanned by the light and the distortions are detected interferometrically. This system has a linear response over 11 orders of magnitude and a spatial resolution limited to the size of the light striking the mirror [16]. The acoustic displacement is not affected by the spectral content of the beam, thus this technique is not frequency-sensitive.

4. Acousto-optic

One of the frequently used techniques for measuring ultrasonic beams involves the interaction of light with sound field. The short theoretical description presented here will follow that of Klein, Cook, and Mayer [17].

A sound beam travelling through a light-transparent medium can be viewed as a regularly spaced series of compressions and rarefactions of that medium. These changes in density result in a small (on the order of one part in 10^5) changes in the refraction index of the medium. Thus a light beam perpendicularly transversing the sound field will "see" an optical phase grating. This interaction of the light with the sound manifests itself as a series of Fraunhofer diffraction orders, where the intensity in the n^{th} order is given by

$$I_n = J_n^2(v) \quad (3.1)$$

where J_n is a Bessel function (of the first kind) of order n . The argument of the Bessel function, v , is given by

$$v = k \left(\frac{\partial u}{\partial p} \right)_s pL, \quad (3.2)$$

where k is the wave number for the light, $(\partial u / \partial p)_s$ is the adiabatic piezooptic coefficient, p is the maximum acoustic pressure and L is the interaction length.

The form of equation (3.1) was first given by Raman and Nath [18] for infinitesimally small amplitudes of of ultrasonic waves in the low MHz-range (up to about 5 MHz) provided the ultrasonic wave is pure sinusoidal.

It was later found [14] that the restrictions on the validity of equation (3.1) as given by Raman and Nath, are not sufficient and that another dimensionless parameter should be considered in analyzing acousto-optic diffraction phenomena; this parameter is given by

$$Q = k^* L / \nu_0 k \quad (3.3)$$

where k^* is the acoustic wave number and ν_0 is the index of refraction of the medium in the absence of sound. The limit of validity of the above theoretical description places the following constraints on Q and v [19]

$$Qv \leq 2, \quad (3.4a)$$

$$Q \ll 2.$$

(3.4b)

When the above conditions are satisfied, equation (3.1) applies, in which case the interaction between light and sound is known as Raman and Nath diffraction.

There is very little energy transferred between the sound and the light during this interaction, leaving the sound field virtually undisturbed during the measurement. An absolute calibration of this technique is accomplished in a rather straightforward manner. By measuring I_n of a given diffraction pattern the Raman and Nath or v parameter can be determined from equation (3.1). With a knowledge of the wave number of the light, the adiabatic piezoptic coefficient and the interaction length, equation (3.2) can be used to determine the acoustic pressure of that part of the beam which interacts with the light.

The above theoretical description assumes a pure sinusoidal acoustic beam. If the acoustic wavefront is distorted (ie., there are harmonics present) the diffraction pattern is no longer described by equation (3.1) [5]. A diffraction pattern is still present, but it is asymmetric about the zero order. From a detailed measurement of all diffraction orders of such an asymmetric pattern one can calculate the harmonic content of the wave form [20,21].

The use of the acoustooptic technique has the advantages that it creates no disturbance of the sound beam during measurement, it is relatively easy to establish an absolute calibration and it is seen to be sensitive to the harmonic content of the beam. One of the obvious disadvantages encountered in using acoustooptic probing is that the information contained in the diffraction pattern represents an integration through the sound field. Thus equation (3.2) is really given by

$$v = K(\partial u / \partial p)_s \int p(L) dL. \quad (3.5)$$

A map of the sound field can be extracted from (3.5) by proceeding as follows. The light beam defines the x-direction and the y-direction is perpendicular to both the light and sound beams. Thus

$$v(y) = K(\partial u / \partial p)_s \int p(x, y) dx \quad (3.6)$$

The function $p(x, y)$ can then be determined from the function $v(y)$ through the use of Fourier projection theory [22]. This procedure requires an a-priori knowledge of $p(x, y)$ and the amount of information to be analyzed is extensive [22].

One limitation of all applications of acoustooptic measurements is the requirement that the measuring system conform to the constraints given by equations (3.4a) and

(3.4b). For low frequencies (less than 5 MHz), low intensities and narrow beam widths, these constraints are easily met. But in the experimental arrangement used here measurements were made sufficiently far from the sound source so that diffraction spreading had increased the value of L . Moreover, harmonic generation had increased the value k^* and consequently the Q parameter no longer obeyed equation (3.4b).

Thus problems encountered when using the acoustooptic technique to map ultrasonic fields are twofold. First, if one uses low MHz frequencies it is quite easy to approach the limits of applicability of the equations (3.4a) and (3.4b). Second, if one wishes to use a two dimensional representation to produce a three dimensional map of the intensity and spectral distribution in the sound field, a method such as Fourier projection theory must be used. This method requires a large amount of information and is not very useful in determining the spectral content.

5. Miniature Hydrophone

The final measuring technique to be examined is electromechanical in nature. If a piezoelectrical crystal (hydrophone) is placed in the ultrasonic field, it responds

mechanically to the variations in pressure at the probe. These mechanical vibrations of the crystal are transformed piezoelectrically into an electric signal which contains information of both the temporal and spatial (with resolution limited to crystal dimension) intensity distribution in the sound field. Since the spatial resolution of the hydrophone is a function of its size, it is clearly advantageous to have the dimension of the probe on the order of wavelength of the sound. The miniature hydrophones used are constructed of a poled ceramic (lead zirconate or barium titanate) sandwiched between two electrodes and mounted in a hypodermic needle [13].

The hydrophone must be calibrated to check response as a function of both incident intensity and frequency. The calibration is most easily done by comparing to one of the other more easily calibrated measuring techniques.

The small dimensions of the miniature hydrophone make it ideally suited for mapping ultrasonic fields. Since the electric signal produced by the hydrophone contains both spectral and intensity information [23], a simultaneous map of the harmonic and intensity distribution in the sound field can be made.

The major limitation in the use of miniature

hydrophones is frequency response [24]. Due to the small size of the ceramic piezoelectric crystal, mechanical mode coupling may occur when the crystal is subjected to several frequencies. Nevertheless, the frequency response of the probe can be accurately determined by careful calibration of the response.

CHAPTER IV
EXPERIMENTAL SETUP

1. Apparatus

The basic experimental apparatus used here consisted of a source of ultrasound and a measuring device capable of mapping the spectral and intensity distribution with the ultrasonic field.

The source of the ultrasonic field was an air-backed quartz transducer 2.5 cm in diameter driven at a frequency of 3 MHz. The transducer was mechanically clamped in a water-tight brass housing leaving an effective radiating area 2 cm in diameter. The transducer was driven from a Westinghouse transmitter, type CAY-52239, modified to supply the necessary high voltage and low current required to drive a quartz piezoelectric device.

The transducer was immersed in a tank of water 120 cm in length, 30 cm wide and 30 cm deep. Sound absorbing rubber was placed in the tank to eliminate reflections from the walls of the tank thus assuring that the ultrasonic field consisted of progressive waves only. The water temperatures remained at 20° throughout the experiment.

The probe used was a miniature hydrophone manufactured by Mediscan Incorporated. The dimensions of the probe are

given in Figure 1. The probe and transducer were mounted on an optical bench above the tank in a manner which allowed three dimensional calibrated motion of the probe with respect to the transducer. The distance between transducer and probe was varied by moving the transducer along the optical bench. With the vertical and lateral adjustments being accomplished by moving the probe in its calibrated holder as shown in Figure 2. Detection of ultrasonic waves with a hydrophone was briefly described in Chapter III. Recall that the probe is constructed such that a piezoelectric crystal intercepts the ultrasonic field and the mechanical deformations it experiences are transformed into an electrical signal. The signal from the probe was transferred via a shielded coaxial cable to a Tektronix IL10 Spectrum Analyzer. The spectrum analyzer consists of a variable frequency (1 to 36 MHz) tuned input circuit coupled to an output amplifier capable of driving a cathode ray tube and a chart recorder. This allows one to Fourier-analyze the electrical output of the probe, yielding the amplitudes of the individual frequency components present in the signal. The spectrum analyzer is phase insensitive; this however, is not a limitation for the present experiment since an a-priori knowledge of the type of signal being analyzed

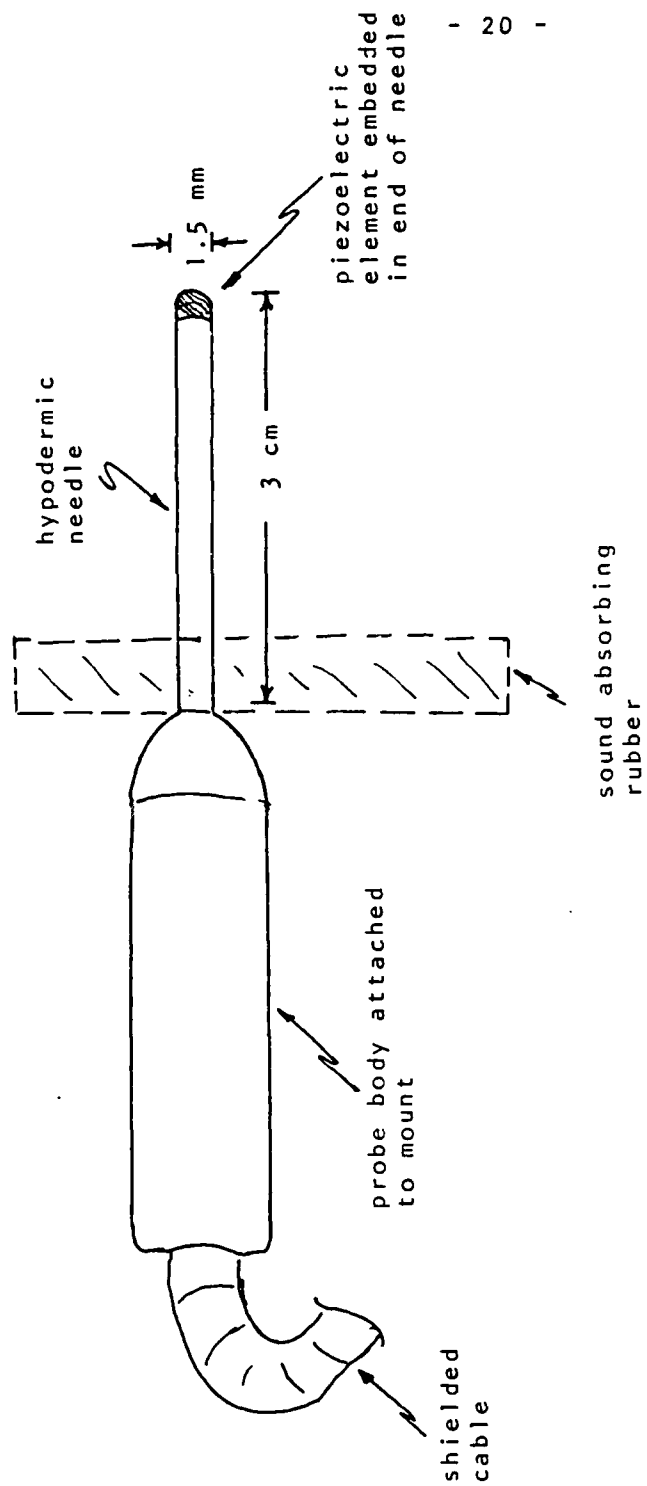


FIGURE 1: Probe dimensions

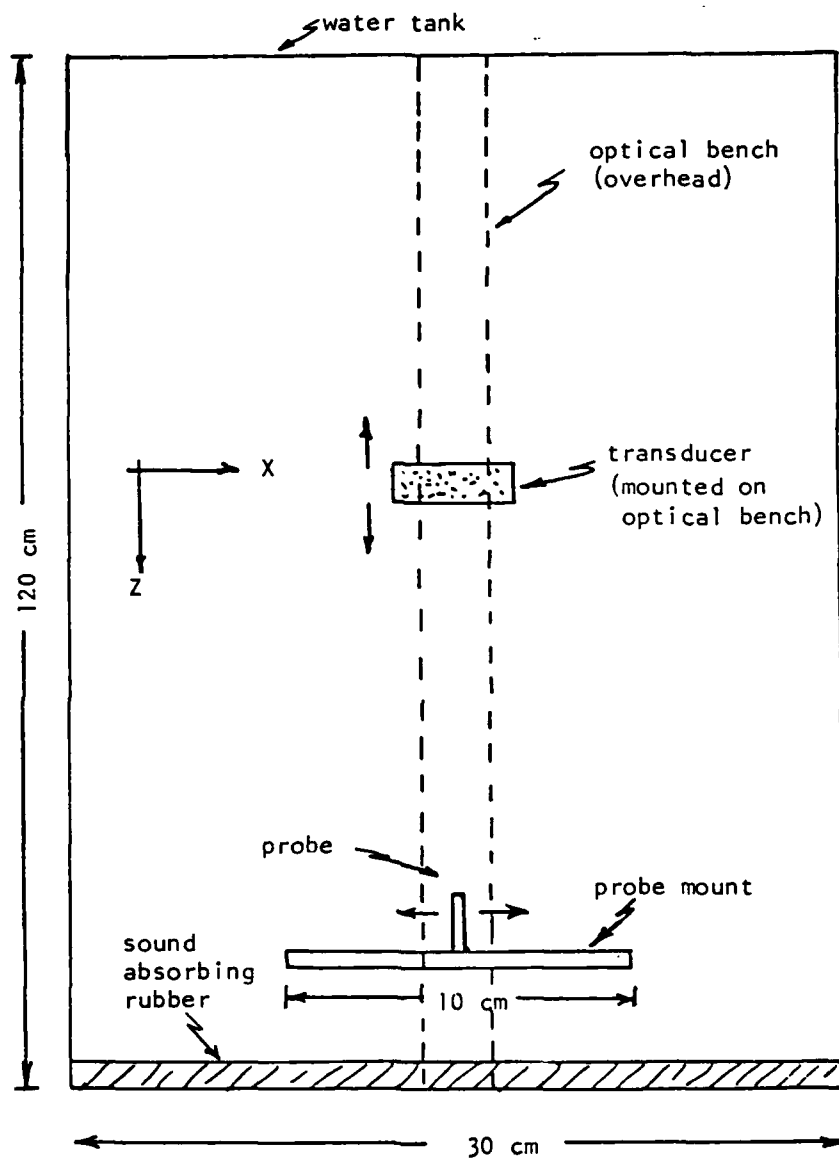


FIGURE 2: Overhead view of probe and transducer mount.

assures one that the phase between the fundamental and the harmonics remains fixed in the progressive wave.

If the response of the hydrophone was flat (i.e., not a function of frequency) then the electrical signal produced by the probe would perfectly replicate the components of the incident acoustic wave. Due to the size limitations placed upon miniature hydrophones, the frequency response is not flat [13,25].

The frequency response of the hydrophone must therefore be measured and the linearity of probe response as a function of incident intensity must also be determined. The calibration procedure is described in the next section.

The second part of the apparatus consisted of an acousto-optic system, shown in Figure 3. It consists of a 5 milliwatt HeNe laser, an optical lens system, an adjustable f stop, and a solid state photo detector. The laser produced a beam of light at a wavelength of 6328 Å. The optical lens system was used to increase the spatial separation of the diffraction pattern in order to facilitate measurement of diffraction order intensities. The f stop was used to reduce the spatial cross section of the laser beam which had been expanded by the lens system. The photo detector was used to determine the amount of light present

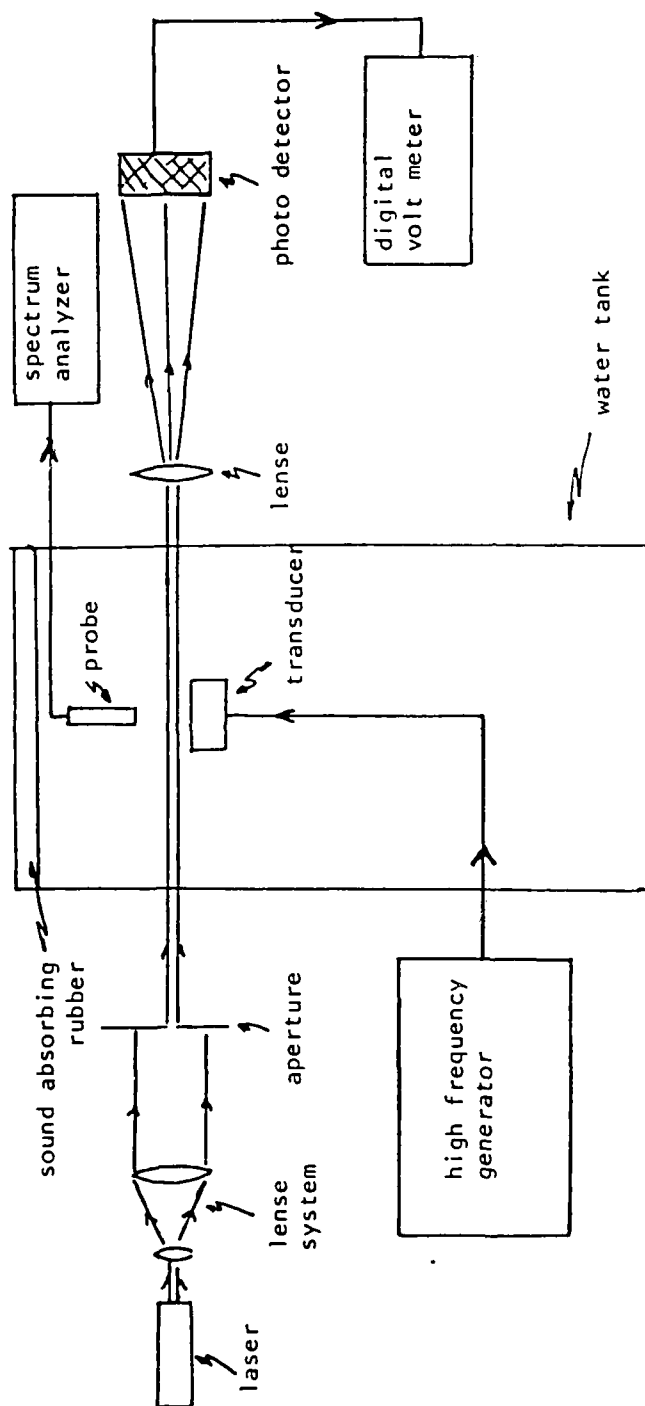


FIGURE 3: Aparatus (block diagram)

in the zero order of the diffraction pattern. This system also required calibration. The procedure is described in the next section.

The experimental arrangement used to map the ultrasonic field was identical to the calibration setup seen in Figure 3, except that the transducer to hydrophone distance was increased.

2. Measurement Procedure

The field of a circular transducer is characterized by means of a dimensionless parameter, α , given by

$$\alpha = \lambda z / a^2 \quad (4.1)$$

where λ is the acoustic wavelength, z is the source-to-probe distance and a is the radius of the transducer. The region from the transducer face, where $\alpha = 0$ to a distance corresponding to $\alpha \approx 1.0$ away from the face is known as the acoustic near field. The region where $\alpha > 1.0$ is known as the acoustic far field.

Measurements were made in a region of the sound field centered around the boundary between the near and far fields. This region was chosen for two reasons. First, an effort was made to provide data taken in an area of theoretical interest where both measurable harmonic components are expected to exist and effects due to other

processes such as diffraction and interference are significant. Second, some work using ultrasonic equipment, for both medical purposes and in scientific research, is performed at these source-to-probe distances, frequently without any specific knowledge of beam intensity distribution or harmonic content existing at these distances.

Six sets of measurements of the ultrasonic field were made at source-to-probe distances varying from 15 cm to 25 cm ($\alpha = 0.75$ to 1.25) in 2 cm increments. At each of the above distances from the transducer a profile was measured at 3, 6, and 9 MHz. An individual profile consisted of 17 measurements made along a 100mm line centered on and perpendicular to the acoustic axis. Each profile was measured four times so that the final profile was an average of the four runs. The amplitude of the ultrasound was set at the beginning of each run such that the diffraction pattern produced with the laser beam 5mm from the face of the transducer had an integrated v value of 2.4 (the first zero of the zero order).

CHAPTER V
CALIBRATION

The miniature hydrophone used to map the ultrasonic field in this experiment required calibration to check both response as function of frequency and linearity of response as a function of incident pressure.

One method of calibrating hydrophone frequency response is to subject the probe to a broad band acoustic pulse and then compare the known spectrum of the acoustic pulse to the measurement spectrum of the hydrophone output [26]. Rather than using this generally accepted method for calibrating the probe, a less involved variation of the technique was employed for two reasons. First, it is not convenient to use this method to test hydrophone linearity. Also, the nature of the acoustic field being measured in this experiment is such that the probe response be known at only certain discrete frequencies. Hence, the hydrophone need only be calibrated at 3, 6, and 9 MHz representing the fundamental and the first two harmonics of the acoustic spectrum, respectively.

1. Calibration Procedure

Calibration runs were made at each of the above three frequencies comparing response of hydrophone and spectrum

analyzer (treated together as one instrument to be calibrated) to simultaneous acousto-optic measurements. The source of the 3 and 9 MHz ultrasonic fields was a 3 MHz transducer driven in its fundamental mode and then at its third harmonic, respectively. The 6 MHz ultrasonic field was produced by driving a 2 MHz transducer at its third harmonic.

Distortion of the ultrasonic waveform due to propagation through the water was minimized during the calibration runs by keeping the transducer-to-hydrophone distance short (approx. 5 mm). This assured that the calibration runs were made on nearly sinusoidal ultrasonic fields. The acousto-optic measurement against which the probe response was calibrated is a measure of the sound pressure in the ultrasonic field that manifests itself in the form of a diffraction pattern. The acoustic pressure can be determined from the diffraction pattern by using equations (3.1) and (3.2). Since only a relative calibration of the response to the three frequencies is under consideration, the probe response was compared to the v parameter (which is proportional to the acoustic pressure through equation (3.2)).

This comparison was made in the following manner:
the hydrophone was placed on the acoustic axis in front of

the transducer and the output voltage of the probe was recorded as the transducer driving voltage was changed. At the same time the laser beam was adjusted so that its optic axis was normal to the acoustic axis with the intercept of the two being between the transducer and the hydrophone as close to the probe as feasible. This arrangement made it possible to probe essentially the same point in the sound field by means of the probe output and the acousto-optic interaction. Varying the transducer driving voltage thus changed both the output voltage of the hydrophone and the light intensity distribution in the light diffraction pattern. The acousto-optic diffraction pattern was analyzed by measuring the zero order light intensity and then using equation (3.1) to determine the appropriate v parameter. As was stated before the acousto-optic diffraction pattern is a measure of the ultrasonic field integrated along the optic axis. Even though the spatial cross section of the laser beam and the active area of the hydrophone were approximately equal, the light beam interacted with more of the sound field than did the probe. But since the distribution of energy in the ultrasonic field near the transducer is not a function of transducer output [19] the diffraction

pattern represents a relative measure of the ultrasonic pressure incident on the probe. That is to say that if the ultrasonic output were doubled, both devices would "see" twice the ultrasonic amplitude. Each of the three calibration runs compared probe response to the acousto-optic v parameter at 13 different ultrasonic intensities. The ultrasonic intensities used for calibrating the probe corresponded to zero order light diffraction intensities ranging from 0.95 ($v \approx 0.3$) to 0.1 ($v \approx 1.8$). Where the total available undiffracted light intensity of the laser has been normalized to one.

2. Calibration Results and Discussion

During the calibration runs, the close hydrophone-transducer proximity was dictated by the need to make measurements at a distance where harmonic distortions of the initial sinusoidal wavefronts have not yet occurred.

Thus, the frequency response calibration of the probe must be done in the near field of the transducer. One problem encountered in making measurements in the acoustic near field is that the amplitude distribution across the beam is not smoothly varying as it is in the far field but is determined by the constructive and destructive inter-

ference of the wavelets emitted by the transducer. An analysis of diffraction patterns produced by the sound field from a circular plane piston source shows fluctuations of as much as 30 percent in the integrated v value for measurements made for different values of α in the near field [26].

In addition to those amplitude variations across the ultrasonic beam, there exists even greater pressure variations along the acoustic axis in the near field. These fluctuations range between zero and twice the initial pressure (i.e. total destructive interference and total constructive interference).

This interference encountered in making measurements in the near field is further complicated by the fact that the minima of the integrated optic effect do not occur at values of α where probe measurements show minima of the pressure along the acoustic axis [26].

Relative calibrations made at one frequency are not affected by this because the laser beam and probe orientation are fixed during a given run. But, the possibility that the relative orientation of hydrophone and laser beam is different for measurements made at different frequencies has the effect of introducing a systematic error into the

frequency calibration data.

This error was minimized in the following way: The frequency calibrations at 3, 6, and 9 MHz were made at transducer-to-hydrophone distances corresponding to a value for α of 0.025, 0.0125, and 0.0083 respectively. The differences in the v values as determined from the diffraction patterns produced by the ultrasonic beam at those values of α were only 2 to 3 percent [26]. Also the pressure variations along the acoustic axis recorded by the hydrophone located at these distances varied by only 10 percent. Thus, a maximum error of 15 percent was assumed for the frequency calibration data.

A graph of probe output versus v value for each of the three frequencies is shown in Figure 4. A straight line was fit to the data for each frequency by Chi squared minimization technique. The calculated slopes of the straight lines are a relative measure of the frequency response of the probe. The response of the probe at 3, 6, and 9 MHz is in the ratio of 1:2.9:3.5 respectively.

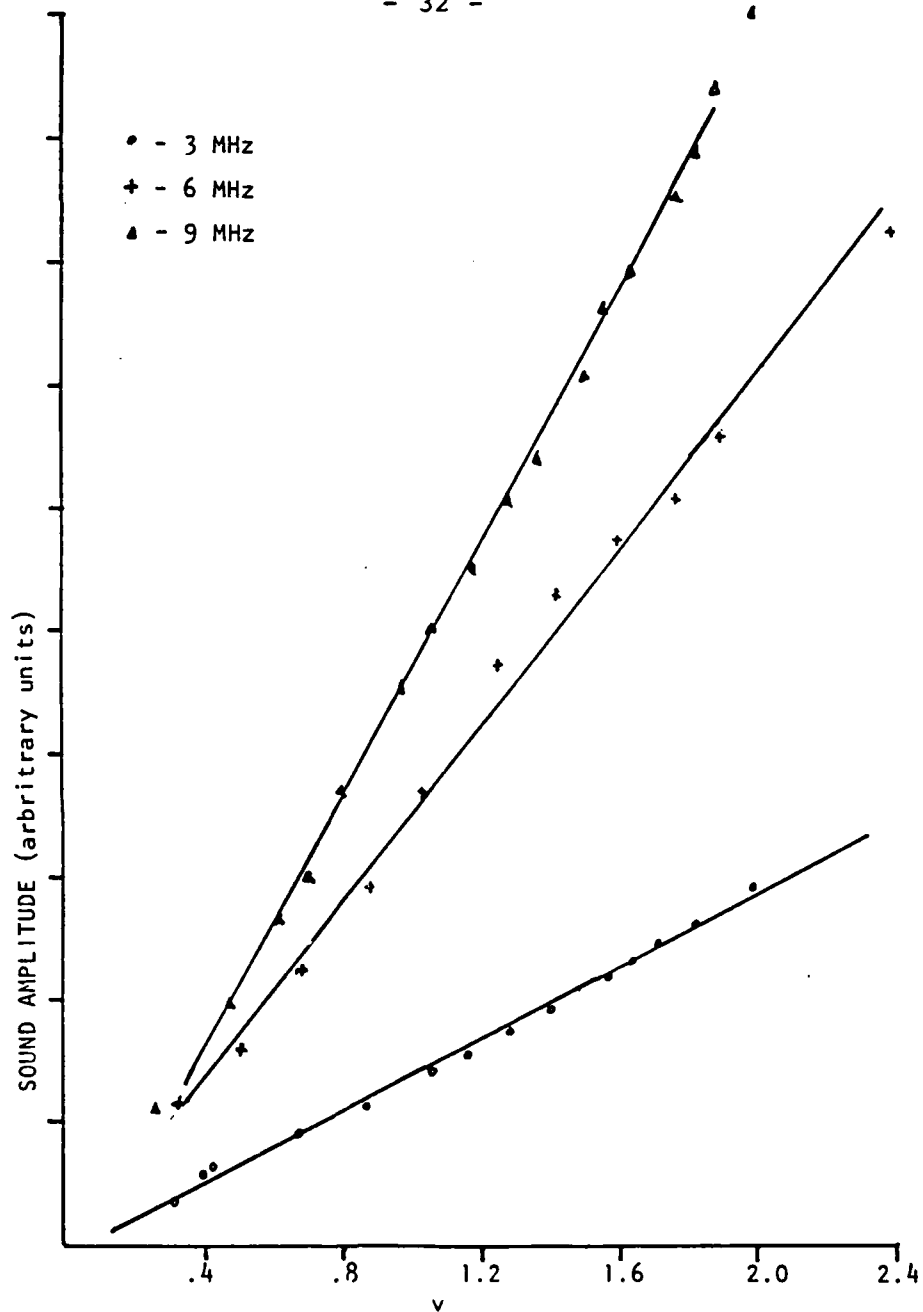


Figure 4: Frequency calibration data. Probe output versus v value.

CHAPTER VI
EXPERIMENTAL RESULTS

The measured ultrasonic profiles, presented graphically in Figures 5 through 10, are grouped for various distances from the source, with each Figure showing the 3, 6, and 9 MHz beam profiles measured at a given distance. The 6 and 9 MHz beam amplitudes have been adjusted to reflect the probe calibration as discussed in Chapter V. Since no attempt was made to correlate probe output to absolute numerical values of ultrasonic pressure, the vertical scale in Figures 5 through 10 is given in arbitrary units. The lines connecting the experimental points in the Figures are merely a visual aid and are not meant to represent a fit to the data.

As was pointed out in Chapter III there is not a comprehensive theory able to predict ultrasonic profiles measured at the source-to-probe distances used here. But, the data can be analyzed in light of the qualitative results predicted by existing theory.

There are many competing processes involved in the determination of these profiles including nonlinear production of harmonics, attenuation, diffraction spreading

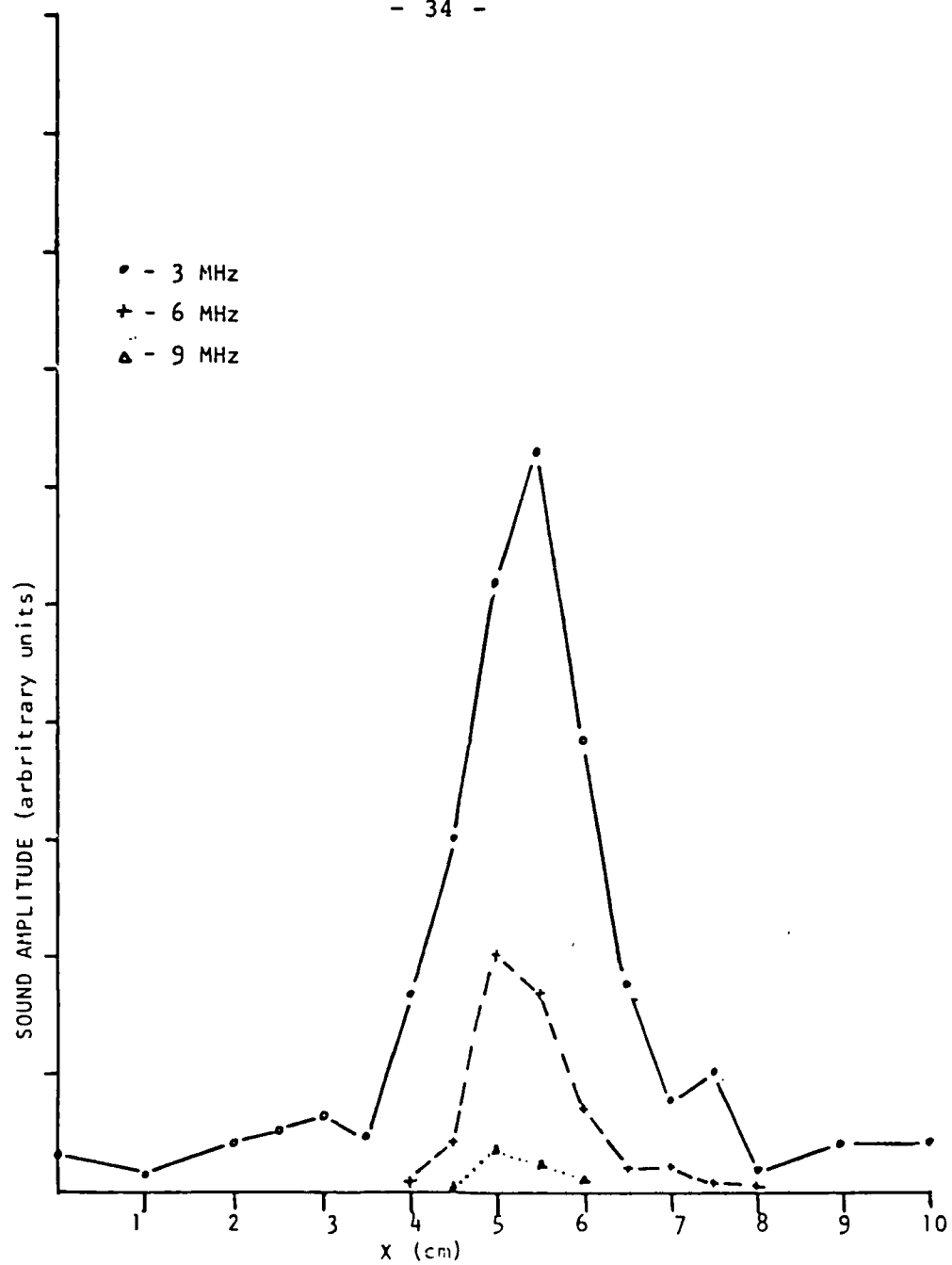


FIGURE 5: Sound amplitude versus distance across sound field for $z = 15$ cm. See figure 2 for a definition of x and z coordinates.

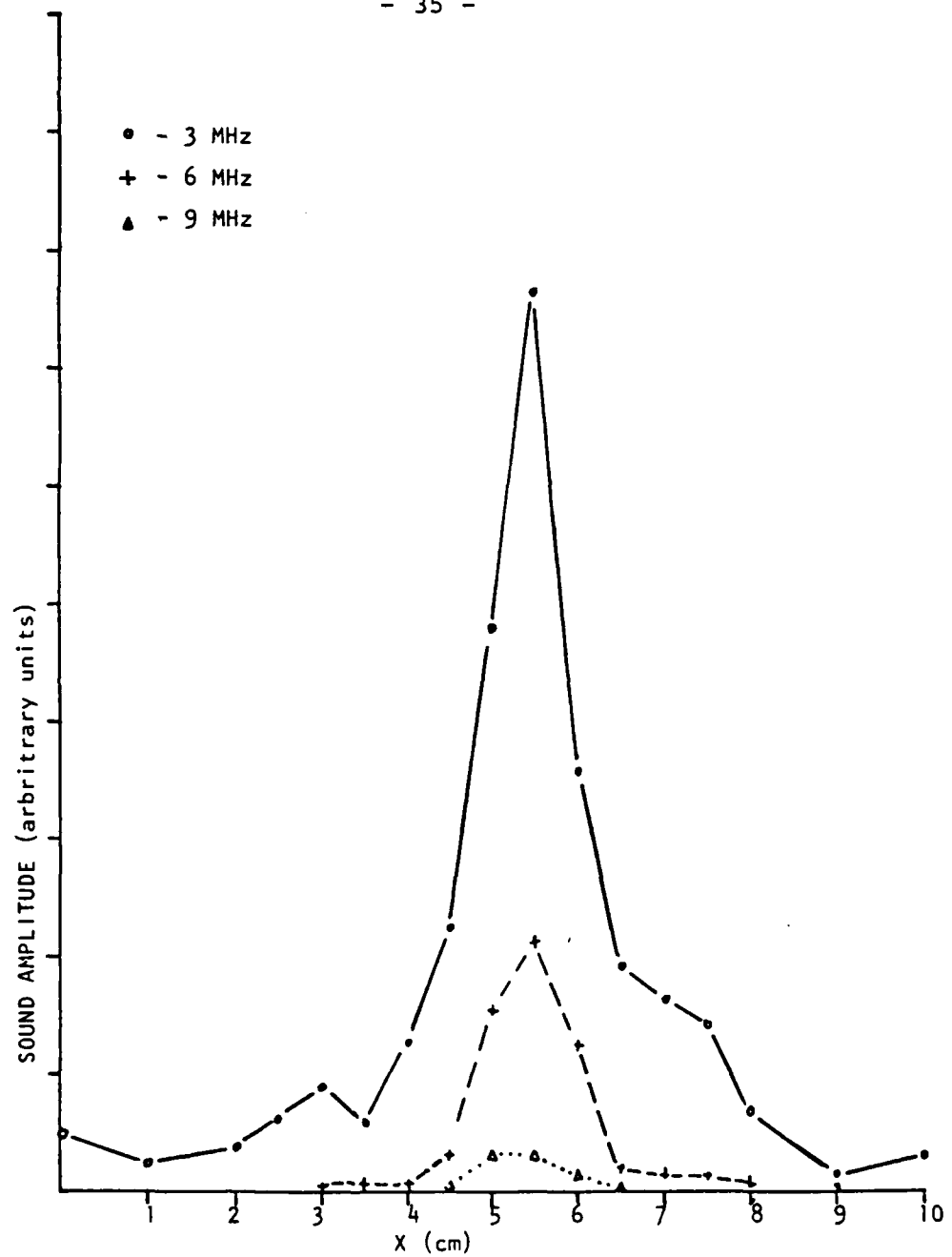


FIGURE 6: Sound amplitude versus distance across sound field for $z = 17$ cm.

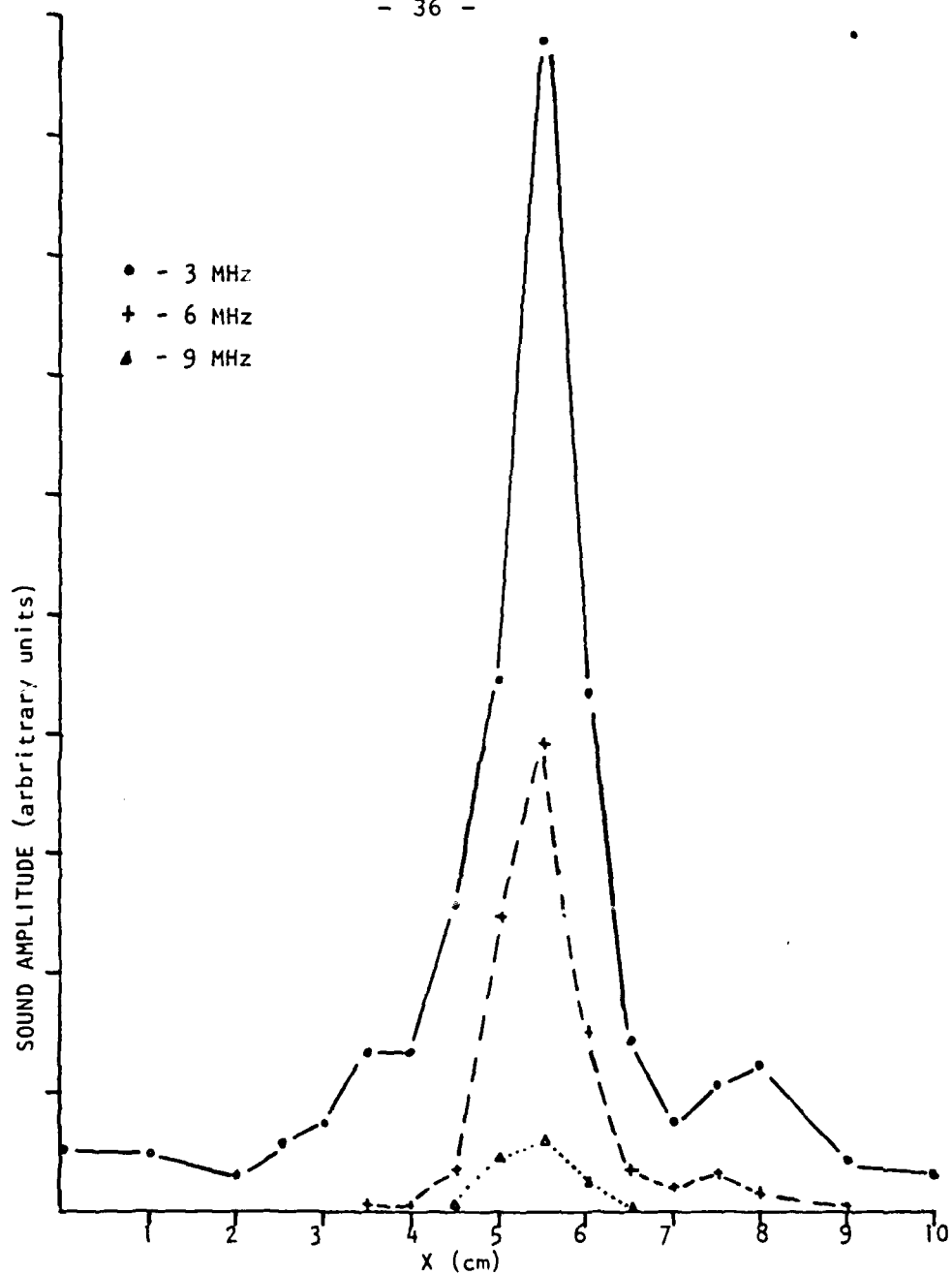


FIGURE 7: Sound amplitude versus distance across sound field for $z = 19$ cm.

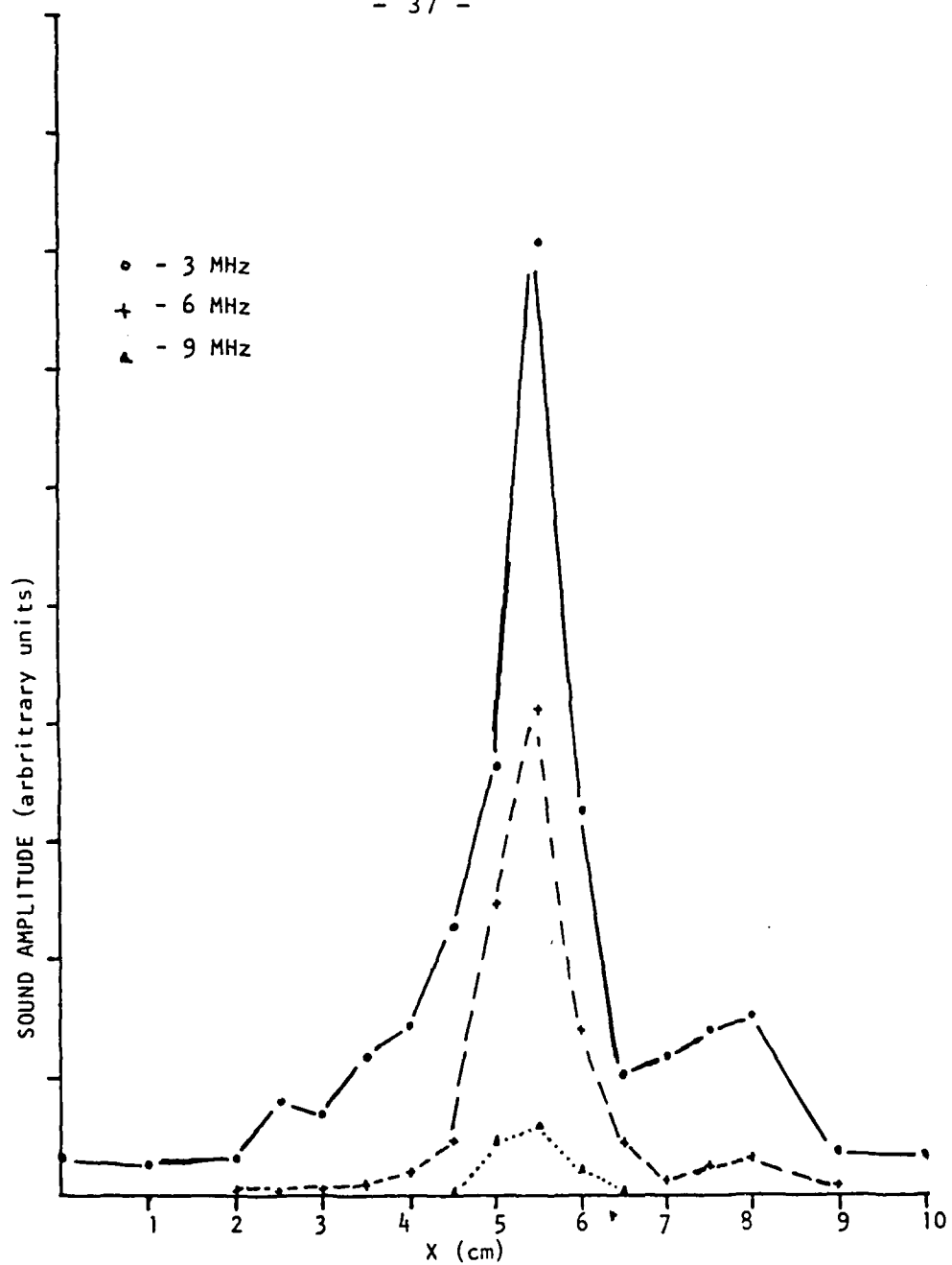


FIGURE 8 : Sound amplitude versus distance across sound field for $z = 21$ cm.

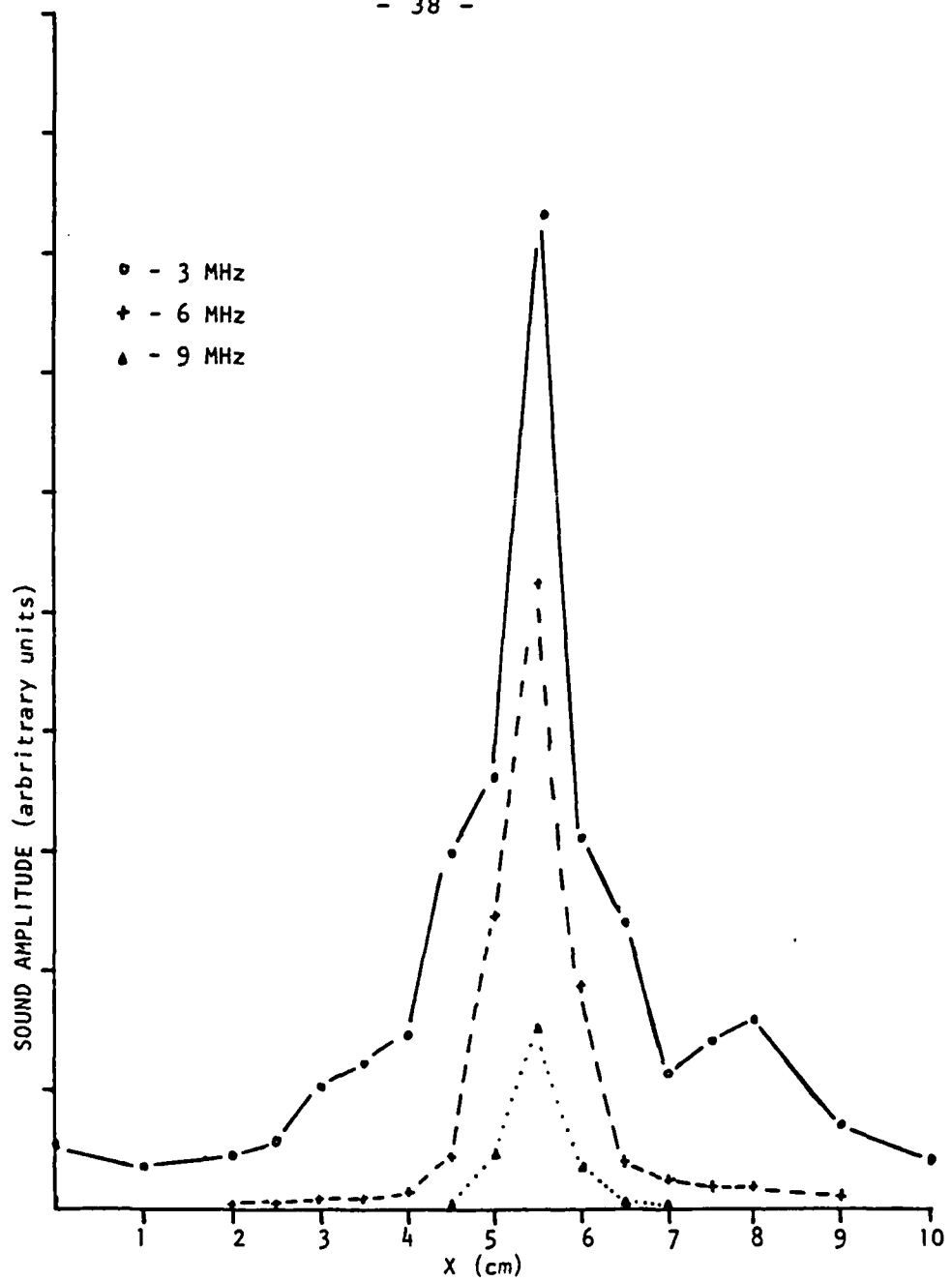


FIGURE 9: Sound amplitude versus distance across sound field for $z = 23$ cm.

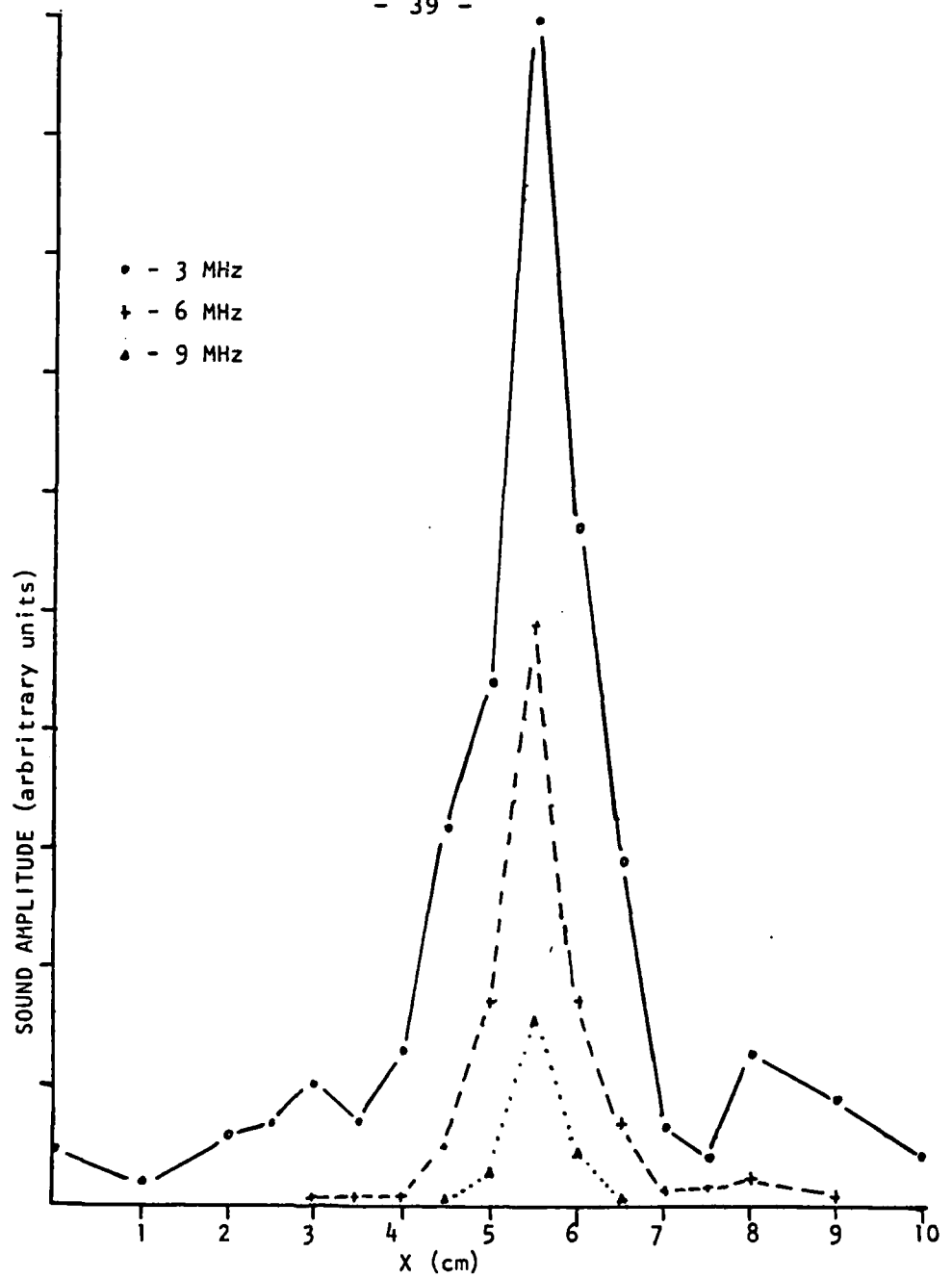


FIGURE 10: sound amplitude versus distance across sound field for $z = 25$ cm.

and interference effects. The fluctuations in maximum amplitude of the 3 MHz beam is an indication that interference affects the profile of the fundamental. It is not clear however, whether the profiles of the first two harmonics are affected by interference. The steady rise of the second and third harmonics as distance from the source increases points to the fact that these profiles are strongly determined by the nonlinear production of the harmonics. The similarity of the profiles at 23 and 25 cm shows that attenuation has balanced harmonic production at this distance for the pressure amplitude initially produced at the source transducer. The lack of a comprehensive analytical expression makes it difficult to determine to what extent the other processes affect the profiles. Examination of the 3 MHz profiles shows that the width (ignoring the tails on either side of the minima) remains constant at the distances considered here. Thus either diffraction spreading is not significant or it is effectively balanced by some other competing processes.

In order to make the measurements more useful for possible future theoretical work, an effort was made to fit an analytic expression to the data. The fit to the data was accomplished using a weighted chi-square minimi-

zation technique [27].

An I.B.M. 360 computer was used to analyze the data. The average ultrasonic amplitudes (shown in Figures 5 through 10) along with the standard deviation (on the mean) for each data point was calculated by the computer. The standard deviation served as the weight factor used in the chi-square fit. The average ultrasonic intensities and the corresponding standard deviation were stored in the computer in a large array so as to facilitate further data minipulation.

Initially an attempt was made to fit a fourth order polynomial to the beam profiles. But, it was determined that the profiles were too highly peaked to be adequately represented by a polynomial of as low an order as four. Thus a higher order polynomial was needed. The immediate problem encountered here was that a higher order polynomial requires that a greater number of independent parameters be fit to the data. And, it is impossible to fit to the data a polynomial which contains more independent parameters than there are data points. As an alternate method to obtain a fit, an analytic expression of the form $A(1-bx^2)^n + C$ was considered. The parameter A, representing the maximum height of the profile,

and the parameter C representing the background, were estimated from the graphical representation of the data as given in Figures 5 through 10. The expression was fit to the data for values of n equal to 2, 4, 6, and 8. Thus for a given value of n there was only one independent parameter to be determined through the chi-square minimization process.

The best fit to the data occurred for n equal to 6. Figure 12 shows the calculated profiles and the experimental points at the probe-to-source distance of 23cm. The minimum value of chi-square obtained through the fitting procedure serves as a statistical measure of how well the analytic expression fits the data. The values of chi-square calculated here were rather large so that little statistical significance can be placed on the expressions as representation of the beam profiles. Nonetheless, some useful information can be extracted from the calculated analytic expressions. The zeroes of $A(1-bx^2)^n$ occur at values of x equal to $\pm \sqrt{1/b}$. Thus, the expression $2\sqrt{1/b}$ is a measure of the width of the beam profiles. Table 1 lists the values of $2\sqrt{1/b}$ as calculated from the above analytic expression for $n=6$. It is noted that the zeros listed in the table

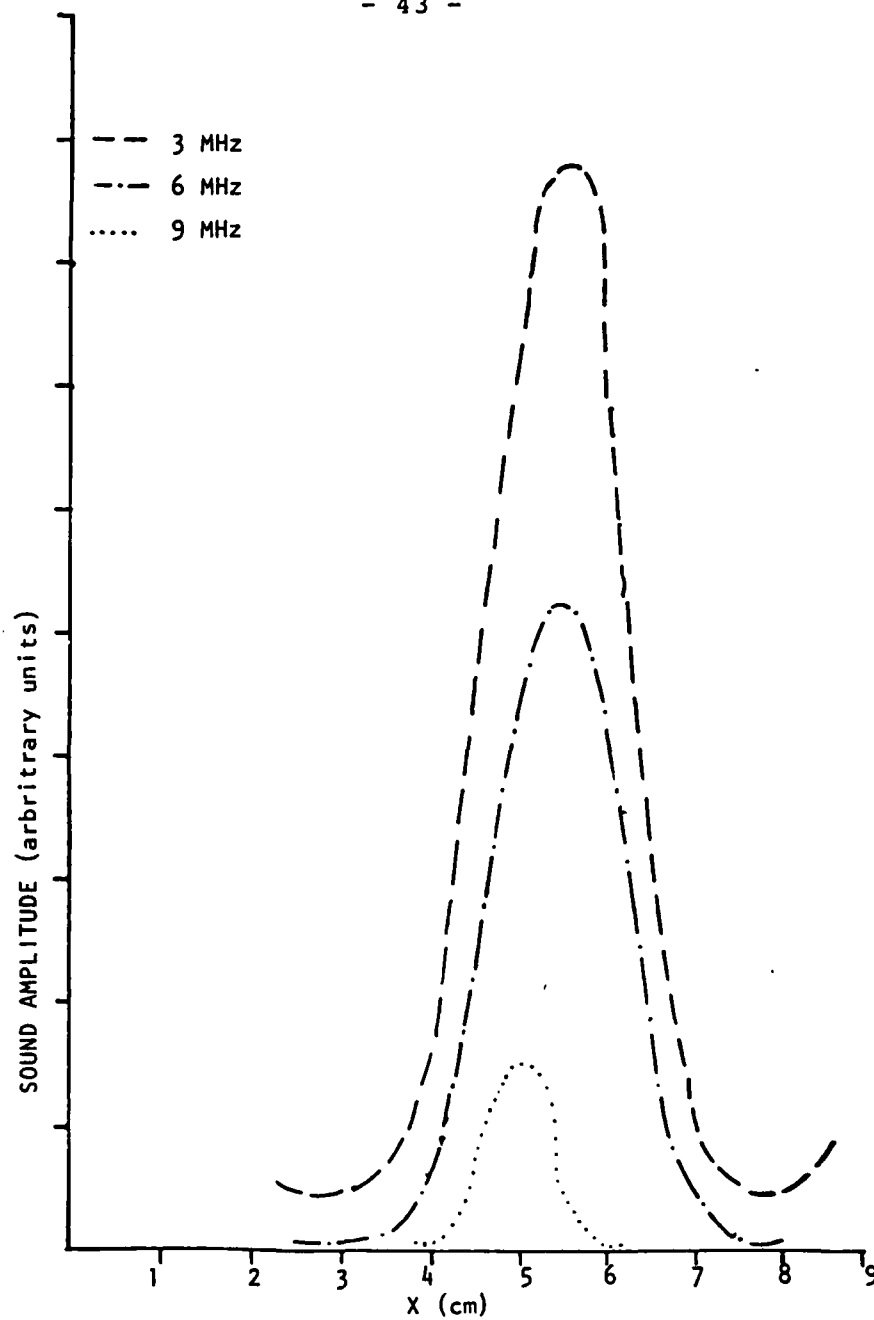


FIGURE 11: Computer fit to data for $z = 23$ cm.

TABLE 1

$2\sqrt{1/b}$ calculated from computer fit
for $n=6$

<div>x (cm)</div> <div>freq.</div>	3 MHz	6 MHz	9 MHz
15	62	42	23
17	59	42	30
19	55	40	28
21	55	41	26
23	55	41	26
25	55	48	24

occur essentially at the same value of x for all the beam profiles at a given frequency, thus further confirming the absence of diffraction spreading. This absence of spreading had already been found experimentally as indicated in Figures 5 through 10.

CHAPTER VII

CONCLUSIONS

The map of the ultrasonic field presented here was made in a region of both theoretical and experimental interest. The data and calculated profiles together with the observations presented in Chapter IV form a basis for future theoretical work. The data may be useful in the study of the interaction of distorted ultrasonic waves with biological systems.

In the work presented here particular attention was paid to the experimental apparatus and the calibration technique employed. The comparison of measuring techniques presented in Chapter III shows the system used here to be the most suitable for this application.

As a suggestion for further work, the probe could be calibrated in absolute rather than relative values, which were used in the present work where the interest lay only in a relative measure of the growth of the harmonics and their percent contribution to the total power in the beam. In the work presented here the interest was in producing an overall mapping of the beam and the number of data points were sufficient to accomplish this task.

As a future effort one could consider measurements which evaluate the sound pressure profile at more closely spaced intervals which would yield more data points to be used in developing the fit to the data. This could yield a better statistical analysis with a corresponding higher level of confidence.

REFERENCES

1. T. G. Muir, "Nonlinear acoustics: A new dimension in underwater sound," in Science, Technology, and the modern Navy, Dept. of the Navy Office of Naval Research, Arlington Va. 1976.
2. R. T. Beyer, Nonlinear Acoustics, Naval Ship Systems Command, Dept. of the Navy, 1974.
3. David G. Crighton, "Model equations of nonlinear acoustics," Ann. Rev. Fluid Mech. 11, 11 (1979).
4. V. P. Kuznetsov, "Equations of nonlinear acoustics," Sov. Phys. Acoust. 16, 467 (1971).
5. K. Zankle and E. Heideman, "Diffraction of light by ultrasonic waves progressing with finite but moderate amplitudes in liquids," J. Acoust. Soc. Am. 31, 44 (1959).
6. V. A. Krassilnikov, V. V. Shklovskaya-Kordy and L. K. Zarembo, "On the propagation of ultrasonic waves of finite amplitude in liquids," J. Acoust. Soc. Am. 27, 624 (1957).
7. David T. Blackstock, "Directive harmonic generation in the radiation field of a circular piston," J. Acoust. Soc. Am. 53, 1148 (1973).
8. Mark B. Moffett, "Measurement of fundamental and second harmonic pressures in the field of a circular piston source," J. Phys. (Paris) C8, 39 (1979).
9. David T. Blackstock, "Propagation of plane sound waves of finite amplitude in nondissipative fluids," J. Acoust. Soc. Am. 34, 9 (1961).
10. D. G. Crighton and J. F. Scott, "Asymptotic solutions of model equations in nonlinear acoustics," Philos. Trans. R. Soc. London, Ser. A: 292, 101 (1979).
11. N. S. Bakhvalov, Ya. M. Zhileikin, E. A. Zabolotskaya and R. V. Khokhlov, "Harmonic generation in sound beams," Sov. Phys. Acoust. 25, 101 (1979).

12. N. S. Bakhvalov, Ya. M. Zhileikin, E. A. Zabolotskaya and R. V. Khokhlov, "Propagation of finite amplitude sound beams in a dissipative medium" Sov. Phys. Acoust. 24, 271 (1978).
13. M. E. Haran, "Visualization and measurement of ultrasonic wavefronts" Proc. IEEE 67, 454 (1979).
14. H. F. Stewart, M. E. Haran and B. A. Herman, "Ultrasonic measurements and calibration" Nat. Bur. Stand. (U.S.), Spec. Publ. 456, 91 (1976).
15. T. Hasegawa and K. Yosioka, "Acoustic-radiation force on a solid sphere," J. Acoust. Soc. Am. 46, 1139 (1960).
16. R. Mezrick, D. Vilkomerson and K. Etaold, "Ultrasonic waves: their interferometric measurement and display," Appl. Opt. 15, 1499 (1979).
17. W. R. Klein, B. D. Cook and W. G. Mayer, "Light diffraction by ultrasonic gratings," Acoustica 15, 67 (1965).
18. C. V. Raman and N. S. N. Nath, "The diffraction of light by high frequency sound waves: part 1," Proc. Indian Acad. Sci. 2, 406 (1935).
19. W. R. Klein and B. D. Cook, "Unified approach to ultrasonic light diffraction," IEEE Trans. Sonics Ultrason. SU-14, 123 (1967).
20. B. D. Cook, "Determination of ultrasonic wavefronts by optical methods," IEEE Trans. Sonics Ultrason. SU-11, 89 (1964).
21. B. D. Cook, "Determination of finite amplitude distortion by light diffraction," J. Acoust. Soc. Am. 32, 336 (1960).
22. B. D. Cook, "Ultrasonic radiation determination by optical methods," Procs. (Biological effects and characteristics of ultrasound sources), H.E.W. Publ. 8048, 99 (1978).
23. W. G. Mayer and E. A. Heideman, "A simple method for the harmonic analysis of an ultrasonic wave," Naturwissenschaften 47, 55 (1960).

24. G. R. Harris, B. A. Herman, M. E. Haran and S. W. Smith, "Calibration and use of miniature ultrasonic hydrophones," Procs. (Biological effects and characteristics of ultrasound sources), H.E.W. Publ. 8048, 169 (1978).
25. R. A. Robinson, "Radiation force techniques for laboratory and field measurements of ultrasonic power," Procs. (Biological effects and characterizations of ultrasound sources), H.E.W. Publ. 8048, 114 (1978).
26. F. Ingenito and B. D. Cook, "Theoretical investigation of the integrated optical effect produced by sound fields radiated from plane piston transducers," J. Acoust. Soc. Am. 45, 572 (1969).
27. Stuart L. Meyer, Data Analysis for Scientists and Engineers, John Wiley and Sons, Inc., New York, 1975.

DA
FIL
2